

# Friction Factors for Spatially Varied Flow with Increasing Discharge

Simon Beecham<sup>1</sup>; Mehdi H. Khiadani<sup>2</sup>; and Jaya Kandasamy<sup>3</sup>

**Abstract:** This paper describes an experimental investigation of how friction factors change for spatially varied flow in sloping channels receiving lateral inflow. The results are compared with those of Beij in 1934, and it is concluded that uniform flow resistance coefficients are not always appropriate for spatially varied flow. Moreover, the common technique of assuming a constant friction factor over the entire length of the channel has been found to have little theoretical justification. The method of Keulegan in 1952 for calculating friction factors in spatially varied flow gives a better estimate, but does not explicitly take account of the lateral inflow rate or velocity. Beij's 1934 experimental data, which was used by Keulegan does not show a systematic variation of friction factor with lateral inflow rate for a constant Reynolds number although this may be due to the low flowrates used. The results of the present study indicate that the friction factor increases with lateral inflow rate for a constant Reynolds number in the experiments that included subcritical and supercritical flow conditions. A method for calculating friction factors which allows for lateral inflow is presented as a precursor to the development of a general method of evaluating friction factors for spatially varied flow with increasing discharge.

**DOI:** 10.1061/(ASCE)0733-9429(2005)131:9(792)

**CE Database subject headings:** Friction factor; Water discharge; Channel flow; Slopes; Flow resistance.

## Introduction

Both the momentum and energy approaches are commonly used to analyze spatially varied flow. The former accounts for external resistance forces due to friction, whereas the latter includes a term for frictional energy losses within a control volume or body of water. For spatially varied flow, the differences between the energy loss term in the energy equation and the friction loss term in the momentum equation were described by Yen et al. (1972).

It is often assumed that the laws of resistance derived for uniform open channel flow can be applied to spatially varied flow as well, although there is little experimental evidence to support this assumption. Izzard (1944), investigating runoff from paved surfaces, found an increase in discharge immediately after the rainfall had stopped.

In this paper we present results from investigations into the frictional characteristics of spatially varied flow in open channels. We consider the behavior of the friction factor in the Darcy-Weisbach equation using the tractive force equation for spatially varied flow, following the method used by Keulegan (1952).

The complete set of one-dimensional flow equations for the prediction of water surface profiles in spatially varied flow has been given by Yen and Wenzel (1970). Fig. 1 shows a typical form of steady, spatially varied flow with increasing discharge.

From the momentum principle it is possible to derive a suitable resistance equation for spatially varied flow with increasing discharge for a channel that has a uniform cross section throughout. The depth of flow is  $h(x)$ , measured above the lowest point in the cross section and normal to the bed,  $x$  is the distance along the channel bed, and  $y$  is the coordinate perpendicular to  $x$  in the vertical plane measured from the channel bed.

The slope of the channel with respect to the horizontal plane is  $S_0 = \sin \theta \approx \theta$ , where  $\theta$  = gutter angle with horizontal plan. This assumes the longitudinal angle of the channel bed with respect to the horizontal plan is small and typically less than  $6^\circ$ . The average velocity over the channel cross section is  $U$ . The lateral inflow is  $q(x)$  with units of volume per unit time per unit length along the  $x$  direction. The lateral inflow has a velocity  $U_L$  at the point of entry to the main channel flow. This velocity is inclined at an angle  $\phi$  relative to the  $x$  direction.

Considering the conservation of mass and momentum, and assuming that the pressure is hydrostatic over the cross section of the channel, the following equation for steady spatially varied flow with increasing discharge can be obtained, Yen and Wenzel (1970):

$$\frac{dh}{dx} = \frac{S_0 - \frac{\tau_{0x}}{\gamma R_r} + \frac{q}{gA}(U_L \cos \phi - 2\beta U) - \frac{U^2}{g} \frac{d\beta}{dx}}{1 - \frac{\beta U^2}{gD}} \quad (1)$$

where  $R_r$  = hydraulic radius;  $\beta$  = momentum correction factor;  $A$  = cross-sectional area of the channel;  $D$  = hydraulic depth; and  $\tau_{0x}$  = boundary shear stress in the  $x$  direction. Eq. (1) involves terms that cannot be evaluated analytically. This equation may be simplified by assuming that the velocity is uniform over the cross section and therefore that the momentum correction factor,  $\beta$ , is equal to unity. Based on these assumptions an equation for the boundary shear stress,  $\tau_{0x}$ , can be written

<sup>1</sup>A/Professor, Univ. of Technology, Sydney, Australia.

<sup>2</sup>Assistant Professor, Isfahan Univ. of Medical Sciences, Isfahan, Iran.

<sup>3</sup>Floodplain Specialist, Dept. of Infrastructure, Planning and Natural Resources, NSW, Australia.

Note. Discussion open until February 1, 2006. Separate discussions must be submitted for individual papers. To extend the closing date by one month, a written request must be filed with the ASCE Managing Editor. The manuscript for this paper was submitted for review and possible publication on April 2, 2004; approved on January 26, 2005. This paper is part of the *Journal of Hydraulic Engineering*, Vol. 131, No. 9, September 1, 2005. ©ASCE, ISSN 0733-9429/2005/9-792-799/\$25.00.

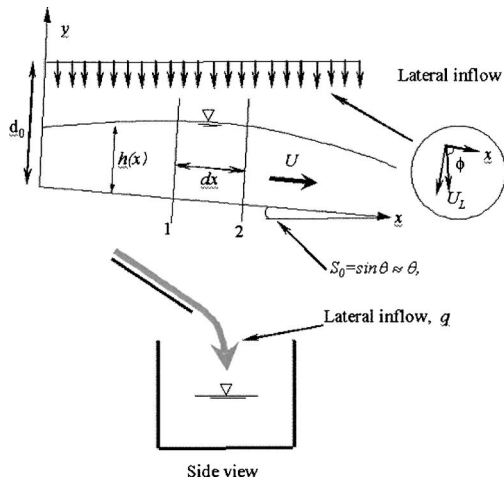


**Fig. 1.** Spatially varied flow with increasing discharge through lateral inflow (for small angles,  $\theta < 6^\circ$ )

$$\tau_{0x} = \gamma R_r \left[ S_0 + \frac{q}{gA} (U_L \cos \phi - 2U) - (1 - F^2) \frac{dh}{dx} \right] \quad (2)$$

in which  $F$ =Froude number defined as  $F=U/(gh)^{1/2}$  for rectangular cross sections only. If the lateral inflow discharges into the channel from a horizontal roof edge (see Figs. 1 and 2) this will have an angle  $\phi$  with the  $x$  direction. Therefore, the stream-wise lateral inflow velocity is given by  $U_L \cos \phi$ . As  $\cos \phi = \sin(\pi/2 - \phi) = \sin \theta$ , the stream-wise velocity is  $U_L \sin \theta$  or  $U_L S_0$ .

### Evaluation of Resistance in Spatially Varied Flow

To analyze Eq. (2), we need to evaluate the boundary shear stress,  $\tau_{0x}$ . The following relationship can be derived from dimensional analysis, Henderson (1966):

$$\tau_{0x} = \xi \rho U^2 \quad (3)$$

where  $\xi$ =dimensional number that depends on parameters including Reynolds number, Froude number, cross-sectional shape, channel slope, lateral inflow rate, and the boundary roughness. The conventional approach in open channel flow analysis is to express the dimensional number,  $\xi$ , in terms of the Manning's, Chezy, or Darcy-Weisbach equations. The following equation (Henderson 1966) describes their respective interrelationships:

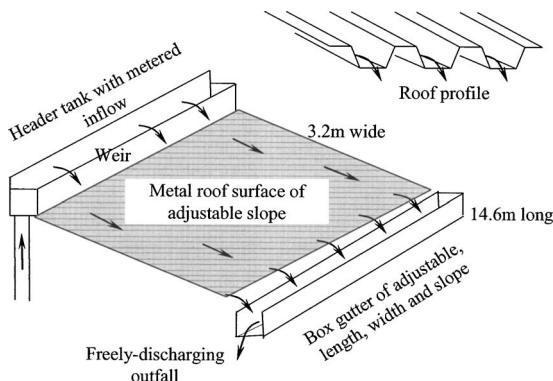


**Fig. 2.** Plan view of experimental apparatus

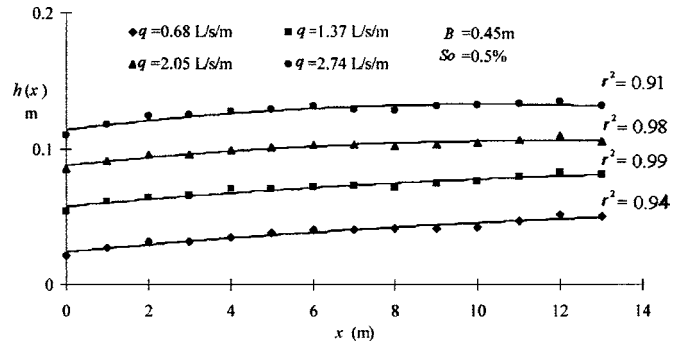


**Fig. 3.** Fitted polynomial curves through measured water depths ( $S_0 = 0.5\%$ )

$$\frac{1}{\sqrt{\xi}} = \frac{U}{\sqrt{\tau_{0x}}} = \frac{\psi R_r^{1/6}}{\sqrt{gn}} = \frac{C}{\sqrt{g}} = \sqrt{\frac{8}{f}} \quad (4)$$

where  $n$  and  $C$ =Manning's and Chezy roughness coefficients, respectively, and  $f$ =Darcy-Weisbach friction factor.

For the special case of steady uniform flow in a channel with impervious fixed boundaries the effects on the behavior of the resistance coefficients has been investigated extensively [for example, see Chow (1959) and Henderson (1966)]. For other types of flow the determination of the resistance coefficients has long been a challenge.

Since the development of Prandtl's boundary layer theory, other formulas have been devised to predict the friction factor,  $f$ , in the Darcy-Weisbach equation. The Blasius, Colebrook-White, and von Karman-Prandtl equations are well-known resistance formulas that can predict the friction factor in the Darcy-Weisbach equation. These formulas give satisfactory results for steady uniform flow in axisymmetric pipes or for flow across flat plates.

The applicability of the above-mentioned resistance formulas in steady uniform open channel flows with small aspect (width to depth) ratios and nonuniform open channel flows is still uncertain. Experiments have shown that when the aspect ratio of the channel is small, secondary currents are generally present. These currents affect the velocity distribution in the channel, which in turn alters the resistance. In spatially varied flow with increasing discharge, strong secondary flows are often present due to the lateral inflow. Therefore, ideally we should calculate the boundary shear stress by direct measurement of velocities in the boundary layer, or calculate the boundary shear stress from Eq. (2). This tractive force equation approach for spatially varied flow was used by Keulegan (1952) to calculate the friction factor,  $f$ , for flow in box gutters using Beij's experimental data (Beij 1934). For estimating the friction factor in sloping gutters, Keulegan gave the following equation:

$$f = \frac{320}{R} \quad (5)$$

in which  $f$ =Darcy-Weisbach friction factor, defined as  $8gR_r S_f / U^2$ , where  $S_f$ =friction slope and the Reynolds number,  $R$ , is defined as  $R_r U / \nu$ , where  $\nu$ =kinematic viscosity.

There are studies where the equations of motion (de Saint Venant equations) were employed to calculate the friction factor or friction velocity (or shear velocity). Tu and Graf (1993) used the de Saint Venant equations to calculate the friction factor in the

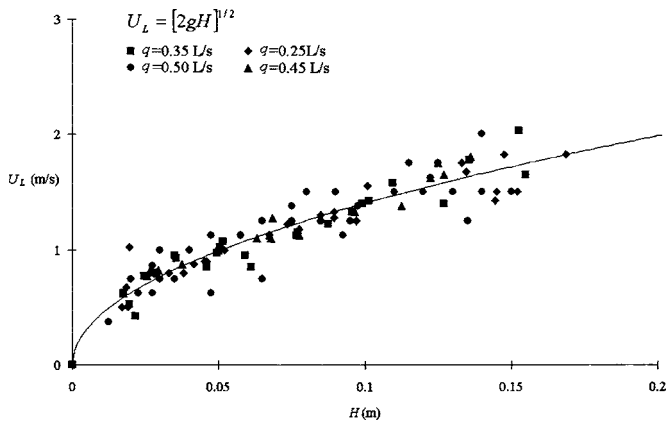


**Fig. 4.** Theoretical and experimental calculation of the vertical component of lateral inflow velocity. Note:  $H=[d_0+S_0x-h(x)]$ .

Darcy–Weisbach equation for unsteady open channel flow. They assumed that the depth-averaged velocity is uniform over the cross section and that pressure is also hydrostatic. Song and Graf (1994) and Graf and Song (1995) calculated the friction velocity in uniform, nonuniform, and unsteady open channel flows using three different methods. They calculated the friction velocity first by measuring velocity profiles near the channel bed using Clauser’s method (Clauser 1956), second by measuring the Reynolds-stress profiles near the channel bed and extrapolating the measurements to the bed, and finally by using de Saint Venant equations. The difference between the estimates from these methods was almost always within 5%. In the current study, the Keulegan method employing Eq. (2) is used to calculate the friction factor in the Darcy–Weisbach equation. Eq. (2) can be rearranged in terms of the friction factor as follows:

$$f = \frac{8gR_r}{U^2} \left[ S_0 + \frac{q}{gA} (U_L \cos \phi - 2U) - (1 - F^2) \frac{dh}{dx} \right] \quad (6)$$

From Eq. (6) the friction factor can be calculated from the slope of the water surface profile obtained from the experimental measurement of depth along the channel.

## Experimental Data

Spatially varied flow experiments in box gutters have been conducted at the University of Technology Sydney as a contribution to the revision of the Australian Standard AS3500.3 (2003) on roof drainage design. These experiments involved measurement of water surface and velocity profiles along a channel with spatially varied flow. The apparatus, shown in Fig. 2, consisted of a roof sheet, 14.6 m wide by 3.2 m long, feeding lateral flow into a 14.6 m long flume. The width of the channel could be varied from 0.3 to 0.6 m in 0.15 m intervals. Flow from both ends of the header tank was fed through a perforated pipe which was installed along its base. The open channel flume was set at slopes of 2.5, 1, 0.67, and 0.5%. The lateral inflow discharges were set at  $q=0.68, 1.37, 2.05, \text{ and } 2.74 \text{ L/s/m}$ .

The experimental setup used in this study involved a channel with a closed upstream end and a freely discharging outlet. Therefore for all tests presented in this paper, there was a zero base flow in the gutter upstream of the lateral inflow.

## Evaluating the Water Surface Gradient

In Eq. (6) it is necessary to know the variation of water depth along a channel ( $dh/dx$ ) to calculate the friction factor. It was found that a second-order polynomial equation can be fitted to the water surface profile and used to calculate the  $dh/dx$  term in Eq. (6). For illustration, fitted curves for  $S_0=0.5\%$  with varying lateral inflows are shown in Fig. 3.

## Evaluating the Lateral Inflow Velocity

A separate experimental setup was used to estimate lateral inflow velocity using a video camera and dye injection. The vertical components of the initial velocities from the roof were small and assumed to be zero, see Fig. 2. Fig. 4 shows the measured vertical velocities and a theoretical line that is calculated from the following equation:

$$U_L = [2g(d_0 + S_0x - h(x))]^{1/2} = [2gH]^{1/2} \quad (7)$$

where  $H=(d_0+S_0x-h(x))$  and  $d_0$ =vertical distance from the starting point of the lateral inflow acceleration to the upstream end of

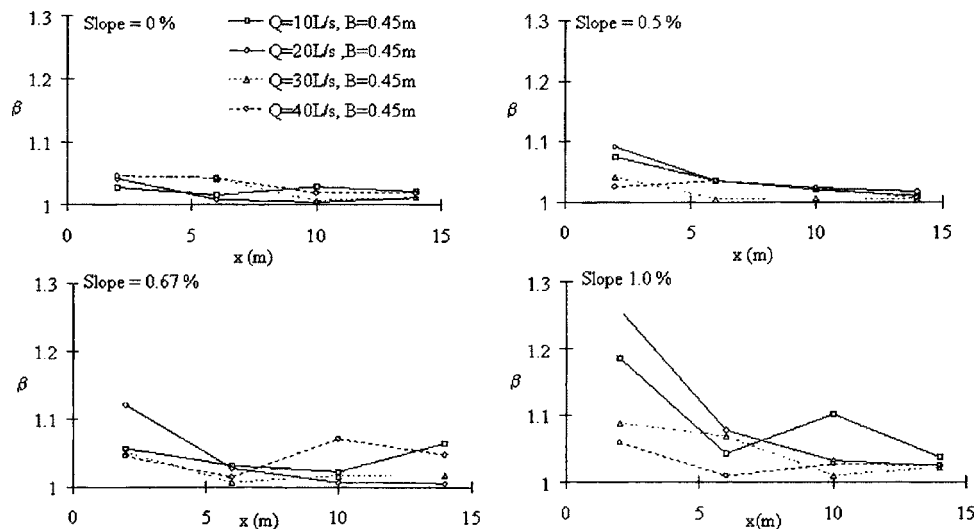


**Fig. 5.** Computed values of momentum correction factor

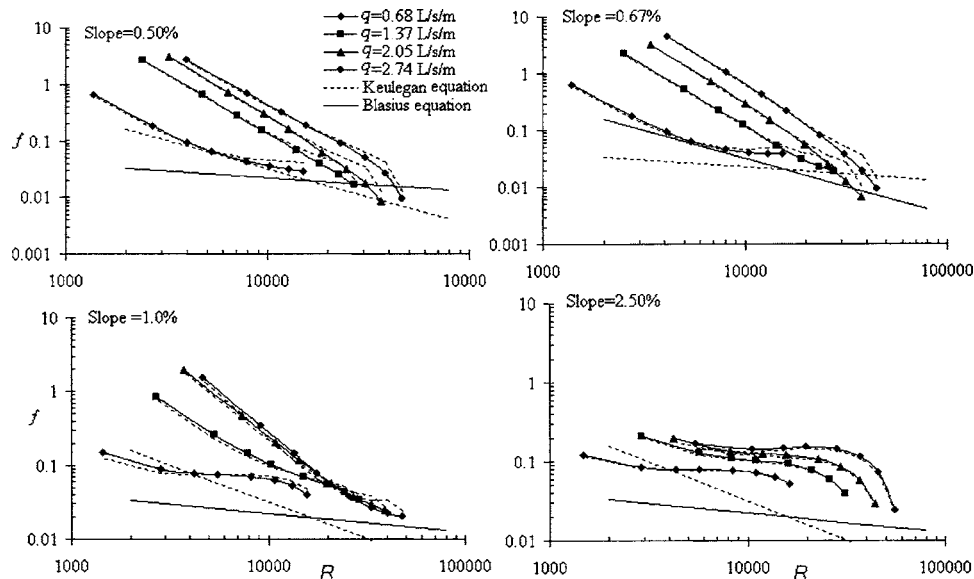


**Fig. 6.** Friction factors versus Reynolds numbers for 0.45 m wide sloping channels. The dotted line plotted beside each data line is for data with friction factors adjusted for  $\beta$ . The dotted line is sometimes obscured by the solid data line because the impact of  $\beta$  is small.

**Table 1.** Computed Friction Factors for 0.45 m Wide Sloping Channel

$q$ (L/s/m)	$x$ (m)	Slope=0.50%			Slope=0.67%			Slope=1.00%			Slope=2.50%		
		F	R	$f$	F	R	$f$	F	R	$f$	F	R	$f$
$q=0.68$	1	0.13	1,367	0.670	0.19	1,397	0.635	0.42	1,440	0.152	0.96	1,470	0.122
	2	0.23	2,705	0.182	0.32	2,768	0.178	0.55	2,838	0.088	1.16	2,908	0.086
	3	0.30	4,018	0.094	0.42	4,114	0.094	0.61	4,200	0.078	1.22	4,319	0.081
	4	0.35	5,308	0.064	0.48	5,436	0.065	0.64	5,533	0.075	1.25	5,706	0.080
	6	0.43	7,827	0.043	0.57	8,011	0.045	0.70	8,134	0.071	1.29	8,424	0.077
	8	0.49	10,281	0.036	0.61	10,500	0.040	0.76	10,683	0.064	1.34	11,091	0.072
	10	0.54	12,687	0.032	0.64	12,908	0.038	0.83	13,219	0.054	1.42	13,732	0.063
	12	0.59	15,058	0.029	0.66	15,241	0.038	0.94	15,777	0.040	1.53	16,370	0.052
$q=1.37$	1	0.07	2,402	2.732	0.10	2,524	2.255	0.18	2,682	0.855	0.66	2,879	0.213
	2	0.12	4,762	0.657	0.18	4,999	0.533	0.30	5,281	0.258	0.85	5,652	0.128
	3	0.18	7,082	0.284	0.25	7,425	0.226	0.39	7,807	0.144	0.92	8,337	0.112
	4	0.22	9,369	0.157	0.31	9,806	0.123	0.46	10,271	0.103	0.97	10,951	0.104
	6	0.30	13,855	0.069	0.40	14,435	0.053	0.56	15,057	0.070	1.05	16,030	0.092
	8	0.38	18,251	0.039	0.47	18,898	0.031	0.64	19,709	0.055	1.14	20,996	0.077
	10	0.44	22,585	0.025	0.52	23,205	0.023	0.71	24,291	0.044	1.26	25,947	0.059
	12	0.51	26,882	0.017	0.56	27,365	0.018	0.80	28,858	0.034	1.44	30,972	0.040
$q=2.05$	1	0.05	3,247	3.101	0.07	3,432	3.263	0.13	3,716	1.947	0.59	4,212	0.196
	2	0.10	6,434	0.717	0.14	6,794	0.741	0.23	7,331	0.472	0.72	8,191	0.133
	3	0.15	9,570	0.297	0.19	10,091	0.299	0.31	10,853	0.208	0.78	11,990	0.124
	4	0.19	12,662	0.158	0.24	13,326	0.152	0.38	14,289	0.118	0.82	15,652	0.120
	6	0.26	18,739	0.063	0.33	19,632	0.055	0.48	20,924	0.058	0.89	22,716	0.107
	8	0.33	24,714	0.032	0.41	25,742	0.025	0.56	27,282	0.038	0.99	29,639	0.086
	10	0.40	30,634	0.017	0.47	31,685	0.013	0.62	33,401	0.029	1.14	36,646	0.058
	12	0.47	36,542	0.008	0.53	37,484	0.007	0.67	39,314	0.025	1.36	43,951	0.029
$q=2.74$	1	0.05	4,001	2.711	0.06	4,119	4.523	0.11	4,676	1.541	0.51	5,495	0.169
	2	0.09	7,931	0.680	0.10	8,152	1.034	0.20	9,179	0.345	0.61	10,561	0.143
	3	0.13	11,804	0.311	0.15	12,107	0.420	0.26	13,529	0.142	0.65	15,314	0.149
	4	0.17	15,635	0.183	0.19	15,992	0.216	0.32	17,740	0.078	0.67	19,844	0.153
	6	0.25	23,227	0.088	0.27	23,575	0.080	0.41	25,808	0.038	0.73	28,526	0.143
	8	0.33	30,812	0.049	0.34	30,950	0.037	0.48	33,486	0.027	0.83	37,097	0.113
	10	0.41	38,494	0.027	0.40	38,162	0.018	0.53	40,859	0.023	0.99	45,973	0.071
	12	0.50	46,375	0.009	0.45	45,249	0.009	0.58	48,000	0.020	1.24	55,571	0.024

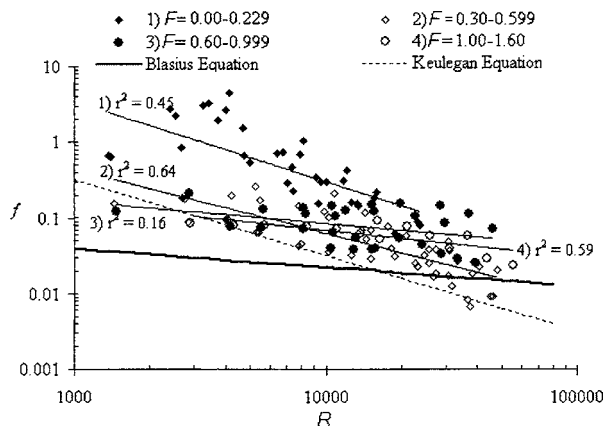


Fig. 7. Effect of Froude number on friction factor

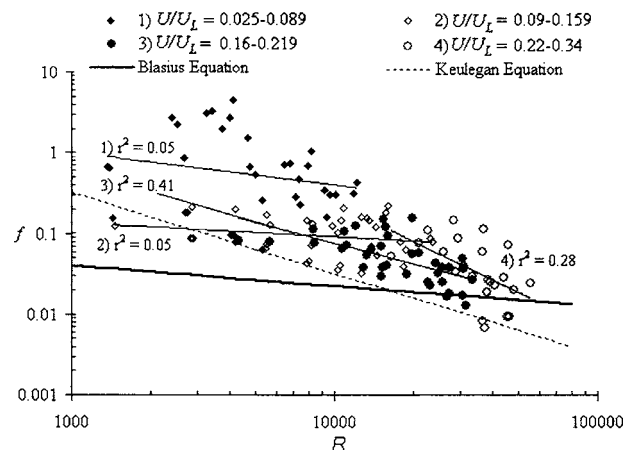


Fig. 8. Effect of relative velocity on friction factor

the channel bed, whereas  $x$ =distance from the upstream end. See Fig. 1.

Fig. 4 shows that the lateral inflow velocities can be estimated reliably using Eq. (7).

## Results

### Evaluating the Momentum Correction Factor

In the derivation of Eq. (6) the momentum correction factor,  $\beta$ , was assumed to be equal to one. This assumption needs to be verified. In contrast to uniform open channel flows, there is little experimental and theoretical work on velocity distributions in spatially varied flow. Hager (1983) reported from Sassoli (1971) that the momentum correction factor,  $\beta$ , in spatially varied flow with increasing discharge depends on the slope of the channel. Sassoli conducted his experiments in a steep, rectangular channel of width 0.15 m, with the slope varying from 5 to 15%, and with a discharge in the range of 5–25 L/s.

The calculated momentum correction factors for the present study have already been presented in Beecham and Khiadani (1996) and are shown in Fig. 5. For different flow configurations, it can be seen that the variation in momentum correction factors is small and most values are close to unity.

### Estimation of Friction Factors and Sensitivity to $\beta$

Knowing the water surface gradients and lateral inflow velocities, the friction factors can now be estimated using Eq. (6). The water surface gradients,  $dh/dx$  were estimated at  $x=1, 2, 3, 4, 6, 8, 10,$  and  $12$  m from the upstream end of the channel. The calculated friction factors are plotted in Fig. 6 and listed in Table 1.

A sensitivity analysis was carried out to determine the sensitivity of  $\beta$  and  $d\beta/dx$  on the friction factor,  $f$ . Values of  $\beta$  and  $d\beta/dx$  given in Fig. 5 were used to calculate friction factors using Eqs. (1), (3), and (4). These friction factors adjusted for  $\beta$  are shown in Fig. 6 as dotted lines and plot very close to the solid data lines that represent the friction factors estimated using Eq. (6) assuming  $\beta=1$ . The dotted lines are sometimes obscured by the solid data lines because the impact of  $\beta$  is small. For the experiments conducted in this study, the impact of  $\beta$  remains small and may be approximated by  $\beta=1$ .

### Friction Factor—Qualitative Trends

Fig. 6 shows the calculated friction factors using Eq. (6). In this figure the Blasius equation and the equation given by Keulegan (1952) are also drawn. The reason for comparing with the Blasius and Keulegan equations is that the Blasius equation represents a lower bound where there is no lateral inflow. The Keulegan equation was developed in conditions where the lateral inflow rates were relatively small.

The friction factor decreases with increasing Reynolds number. Fig. 6 also shows that the calculated friction factors are much higher than the lines representing the Blasius and Keulegan equations. For individual slopes, Fig. 6 also shows that the friction factor appears to depend on the lateral inflow rate. In other words, for a constant Reynolds number the friction factor increases with increasing lateral inflow rate. However, Keulegan's equation derives from Beij's data that do not show any dependency of the friction factor with discrete values of lateral inflow. The reason for this may be due to the low lateral inflow rates used by Beij (1934). The maximum lateral inflow rate in Beij's experiments was 0.56 L/s/m whereas in the current author's experiments the lateral inflow rates varied between 0.68 and 2.74 L/s/m. It can be seen that for the minimum lateral inflow rate of 0.68 L/s/m, the calculated friction factors are in general agreement with the Keulegan equation. However, this is not the case for larger lateral inflow rates.

For  $S_0=2.50\%$ , which include all the supercritical data, see Table 1, the results in Fig. 6 show that for low Reynolds number values ( $R < 10,000$ ) the estimated friction factors are lower when compared to other slope configurations. In contrast for larger Reynolds numbers (say  $R > 10,000$ ) the friction factors are larger. Further studies would be required to determine whether channel slope has an influence on the estimated friction factors.

In summary the experimental data shows that friction factors decline with higher Reynolds numbers, except for supercritical flow and increase with larger lateral flow rates.

### Friction Factor—Quantitative Trends

The friction factors in spatially varied flow might also depend on the Froude number, the relative magnitude of lateral inflow rate to lateral inflow velocity and the relative magnitude of the channel velocity to the lateral inflow velocity.

The effect of the Froude number in open channel flows with no lateral inflow has been investigated extensively. From experi-

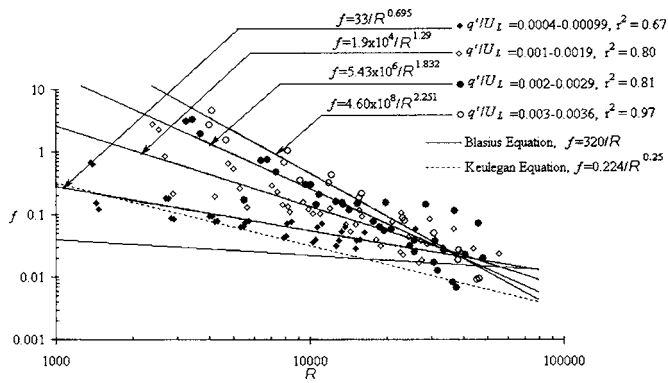


Fig. 9. Effect of relative lateral inflow rate on friction factor

ments conducted in smooth open channel flows, Powell (1946) found no effects of the Froude number on the friction factor for  $F < 1.69$ . Rouse (1963) argued that Froude numbers greater than one influence the friction factor. Iwagaki (1952), analyzed the data of many researchers and concluded that the resistance to flow is influenced by Froude numbers greater than 0.89, when the Froude number is expressed in terms of hydraulic radius. Sarma and Syamala (1991) investigated supercritical flow in smooth open channels. They concluded that for stable supercritical flows, the friction factor varies with the Reynolds number only, as for subcritical flows. For unstable supercritical flows, they found that the friction factor varies according to an equation developed by Rouse.

Yen et al. (1972) investigated the friction factor in laminar sheet flow under rainfall that results in spatially varied flow using the experimental data of Yoon and Wenzel (1971). It was pointed out that the Froude number has only a small effect on the friction factor in laminar sheet flow under rainfall. On the other hand, the rainfall intensity had a larger effect on the friction factor compared to other parameters such as Froude number, rainfall velocity and rain-drop diameter. Beij's experimental data show that the calculated friction factors are more Reynolds number dependent.

The influence of the Froude number, the relative magnitude of velocity in the channel to lateral inflow velocity ( $U/U_L$ ) and the relative magnitude of lateral inflow rate per unit area to lateral inflow velocity ( $q'/U_L$ ) are shown in Figs. 7–9 using the results of the present study. The data points on these figures are classified according to the range of dimensionless groups,  $F$ ,  $U/U_L$ , and  $q'/U_L$  within which they lie. The following observations are made of Figs. 7–9.

- In Figs. 7–9 the Keulegan equation represents the lower bound to the data set. The friction factor increases with larger lateral inflow rates, in some cases by as much as a hundred times over that predicted by the Keulegan equation.
- Figs. 7 and 8 shows that where  $F$  or  $U/U_L$  are low, the friction factor is high. In these cases the average channel velocity is small, and the lateral inflow (that discharges into the main channel as a row of jets) can penetrate further into the channel flow. This is likely to set up strong secondary flow currents, causing a higher resistance and larger friction factor. However the data within each range of  $F$  or  $U/U_L$  display a large scatter. A regression analysis on the data showed that the trend is inconsistent with low regression coefficients. This implies that the parameters  $F$  and  $U/U_L$  are not necessarily good descriptors of the variation in friction factor.
- Where  $F > 1$ , shown in Fig. 7, in supercritical flow, the limited data set shows that estimated friction factors are fairly constant even as Reynolds number increases. A wider range of data is required to substantiate this finding.
- Fig. 9 shows that the friction factor increases in a systematic manner with the relative lateral inflow rate ( $q'/U_L$ ). The data for each range of  $q'/U_L$  are represented by regression lines whose equations and regression coefficients are shown in Fig. 9. These show that, for data collected in the present study, the Reynolds number and the relative lateral inflow rate are good descriptors of the friction factor. This is consistent with the deductions from Fig. 6 outlined in the preceding section. It should be noted that the apparent convergence of lines in Fig. 9, near the region  $R \approx 10^4$ , is simply a result of the regression analysis and resultant straight regression lines and not necessarily representative of the data in that region. Note too that

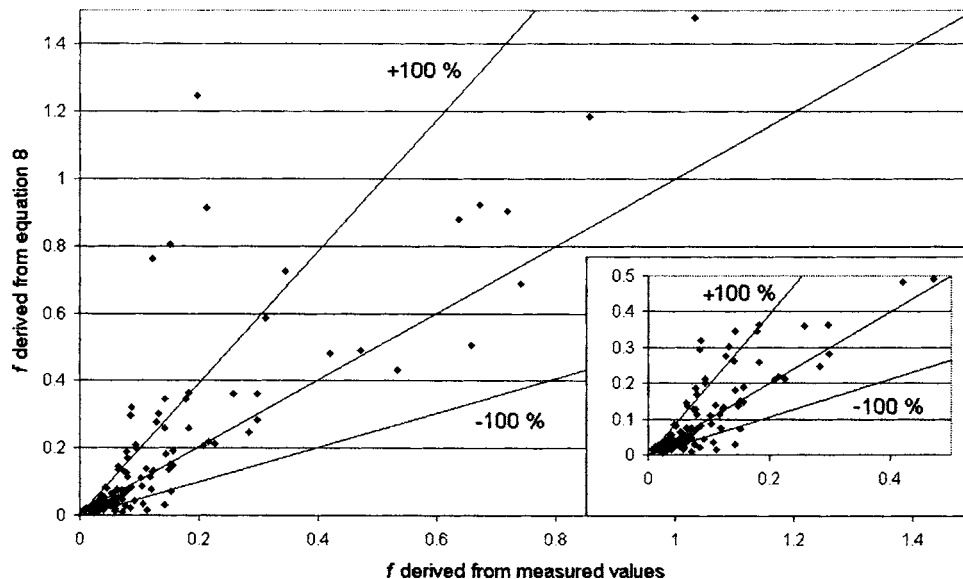


Fig. 10. Comparison of  $f$  predicted from Eq. (8) to that derived from measured values; (inset) the same plot to a larger scale

these observations are limited to the range of lateral inflow used in the experimental study.

The regression equations shown in Fig. 9 can be generalized into the following equation:

$$f = \frac{k}{R^\alpha} \quad (8)$$

where

$$k = 10^{(2.500q'/U_L+2.5)}$$

$$\alpha = \left[ 520 \frac{q'}{U_L} + 1 \right]$$

Note that the Keulegan equation is a lower bound to Eq. (8). The Keulegan equation was developed in conditions where the lateral inflow rates were relatively small. Eq. (8) has been developed for yet higher lateral inflow rates though it should be noted that its application is still limited to the range of lateral inflow used in the experimental study.

The agreement between the friction factors derived using Eq. (6) from the measured values including the water surface gradient  $dh/dx$ , to the those calculated from Eq. (8) is shown in Fig. 10. This figure is plotted in natural scale. Also shown are the  $\pm 100\%$  limits. Fig. 10 shows that the majority of the data are adequately represented by Eq. (8) within the  $\pm 100\%$  bounds. Eq. (8) is preliminary in nature and needs to be tested against data from a wider range of conditions, including supercritical flow, to determine the range of its applicability and what other parameters can significantly influence the friction factor for open channel flow receiving lateral inflow. Eq. (8) is presented as a precursor to the development of a general method of evaluating friction factors for spatially varied flow with increasing discharge.

## Conclusions

The data collected from experiments carried out in roof drainage gutters in the present study shows that the laws of resistance for steady uniform open channel flow do not appear to adequately describe friction loss in spatially varied flows. The empirically derived equation presented by Keulegan (1952) provides a closer approximation, but still underestimates the friction factors for the experimental results of the present study. Keulegan's equation was formulated on the basis of Beij's experimental data, which involved low lateral inflow rates. The results of the present study include data for higher lateral inflow rates. These data indicate that the friction factors are dependent on the Reynolds number and the relative lateral inflow rate ( $q'/U_L$ ). The relationship described by Eq. (8) is preliminary in nature and should be tested for a wider range of data. It is presented as a precursor to the development of a general method of evaluating friction factors for spatially varied flow with increasing discharge.

## Notation

The following symbols are used in the paper:

- A = channel cross-section area;
- B = channel width;
- C = Chezy resistance coefficient;

- $d_0$  = vertical distance from the lateral inflow supply point to the channel bed at the upstream end of the channel;
- F = Froude number;
- f = Darcy–Weisbach resistance coefficient;
- g = gravitational acceleration;
- H = vertical distance from roof edge;
- $h(x)$  = depth of flow section;
- k = coefficient used in Eq. (8);
- n = Manning's resistance coefficient;
- Q = main flow discharge;
- q = lateral flow rate per unit length of channel;
- q' = lateral inflow rate per unit area of channel;
- R = Reynolds number;
- $R_r$  = hydraulic radius;
- $S_f$  = friction slope;
- $S_0$  = longitudinal slope;
- U = average longitudinal velocity over the channel cross section;
- $U_L$  = velocity of lateral inflow;
- x = longitudinal coordinate along the channel bottom direction;
- y = coordinate perpendicular to x in the vertical plane measured from channel bottom;
- $\alpha$  = exponent used in Eq. (8);
- $\beta$  = momentum coefficient;
- $\gamma$  = specific weight of fluid;
- $\theta$  = angle between channel bottom and horizontal plane;
- $\nu$  = kinematic viscosity;
- $\rho$  = mass density of fluid;
- $\tau_{0x}$  = boundary shear stress along x direction;
- $\phi$  = angle between velocity vector of lateral flow and direction of main channel flow; and
- $\Psi$  = a coefficient which depends on the system of units ( $=1 \text{ m}^{1/2} \text{ s}^{-1}$  or  $1.49 \text{ ft}^{1/2} \text{ s}^{-1}$ ).

## References

- Beecham, S. C., and Khiadani, M. H. (1996). "Frictional characteristics of spatially varied flow." *Proc. 7th Int. Conf. on Urban Storm Drainage*, IAHR/IWA, Hanover, Germany, 67–72.
- Beij, K. H. (1934). "Flow in roof gutters." *U.S. Dept. of Commerce, Bureau of Standards: Research Paper RP644, Bureau of Standards J. Res.*, 12, 193–213.
- Chow, V. T. (1959). *Open-channel hydraulics*, McGraw-Hill, New York.
- Clauser, F. (1956). "The turbulent boundary layer." *Adv. Appl. Mech.*, 4, 1–51.
- Graf, W. H., and Song, T. (1995). "Bed shear stress in non-uniform and unsteady open-channel flow." *J. Hydraul. Res.*, 33(5), 699–704.
- Hager, W. H. (1983). "Open channel hydraulics of flows with increasing discharge." *J. Hydraul. Res.*, 21(3), 177–193.
- Henderson, F. M. (1966). *Open channel flow*, Macmillan, New York.
- Iwagaki, H. (1952). "On the law of resistance to turbulent flow in smooth open channels." *Proc. 4th Japanese Nat. Congress for Applied Mechanics*, Science Council, Tokyo, 245–250.
- Izzard, C. F. (1944). "The surface-profile of overland flow." *Trans., Am. Geophys. Union*, 24(6), 959.
- Keulegan, G. H. (1952). "Determination of critical depth in spatially variable flow." *Proc., 2nd Midwestern Conf. on Fluid Mechanics*, Bulletin 149, Ohio State Univ., Engineering Experiment Station, Columbus, Ohio, 67–80.
- Powell, R. W. (1946). "Flow in a channel of definite roughness." *Trans-*

- actions of the ASCE, New York, 531–554.
- Rouse, H. (1963). “Critical analysis of open channel resistance.” *J. Hydraul. Div., Am. Soc. Civ. Eng.*, 91(4), 1–26.
- Sarma, V. N., and Syamala, P. (1991). “Supercritical flow in smooth open channels.” *J. Hydraul. Eng.*, 117(1), 54–63.
- Sassoli, F. (1971). “Canali collettori laterali a forte pendenza.” *Energ. Elettr.*, 36, 26–39.
- Song, T., and Graf, W. H. (1994). “Non-uniform open-channel flow over a rough bed.” *J. Hydrosoci. Hydr. Eng.*, 12(1), 1–25.
- Standard Australia Publications (2003). “Plumbing and drainage—stormwater drainage.” *AS3500.3*, Sydney Australia.
- Tu, H., and Graf, W. H. (1993). “Friction in unsteady open-channel flow over gravel beds.” *J. Hydraul. Res.*, 31(1), 99–110.
- Yen, B. C., and Wenzel, H. G. (1970). “Dynamic equations for steady spatially varied flow.” *J. Hydraul. Div., Am. Soc. Civ. Eng.*, 96(3), 801–814.
- Yen, B. C., Wenzel, H. G., and Yoon, N. Y. (1972). “Resistance coefficients for steady spatially varied flow.” *J. Hydraul. Div., Am. Soc. Civ. Eng.*, 98(8), 1395–1410.
- Yoon, N. Y., and Wenzel, H. G. (1971). “Mechanics of sheet flow under simulated rainfall.” *J. Hydraul. Div., Am. Soc. Civ. Eng.*, 97(9), 1367–1386.